MECHANICAL BEHAVIOUR OF A PERMEABLE BASE AND BEDDING MATERIAL AND THE RUTTING BEHAVIOUR OF PERMEABLE CBPS IN WHICH THEY ARE APPLIED

M. Huurman
Road and Railway Engineering Research Laboratory
Delft University of Technology
P.O. Box 5048
2600 GA Delft, The Netherlands
T +31 15 2781525, F +31 15 2783443
m.huurman@citg.tudelft.nl

W. Boomsma
Aquaflow BV
P.O. Box 58103
1040 HC Amsterdam, The Netherlands
T +31 320 241816, F +31 20 4808061
wboomsma@wxs.nl

SUMMARY

In the Netherlands conditions are not always favourable to civil engineers. The western and northern parts of the country are below sea level. Water management is a constant concern in these regions. Due to climate change and ongoing urbanisation the need for water storage capacity has increased in the last decades. Permeable pavements with a capacity to store and infiltrate water can contribute to solve some of the Dutch problems related to water. Permeable pavements should of course have ample bearing capacity to serve traffic.

This paper discusses a research into the rutting behaviour of the Aquaflow permeable CBP system. First of all laboratory tests were done on the bedding and base material applied in the permeable CBP. By means of triaxial tests the stress dependent stiffness, strength and permanent deformation behaviour of the materials was determined.

Thereafter the behaviour of the permeable CBP was determined on the basis of numerous structural analyses. The analyses give the rutting behaviour of the permeable CBP. More important perhaps is that the analyses give insight into the distribution of stiffness and stress throughout the substructure. With this, insight into the mechanisms that play a role in rutting is obtained. From this insight the designs of permeable CBPs may be adjusted to increase the bearing capacity.

The paper shows that especially the open-graded base material has relatively low cohesion, which reduces the bearing capacity of the CBP. However, it was shown that especially the cohesion of the base material increases with compaction. Proper compaction thus increases the baring capacity of the permeable CBP.

It was shown that the Aquaflow permeable CBP system can be constructed so that a pavement with ample bearing capacity is obtained. Demands with respect to levels of in-situ base compaction are indicated. Depending on base thickness and load magnitude a minimum degree of compaction is defined.

Results of accelerated pavement tests on permeable CBPs reported by Atkinson and Blackman (2001) indicate the accuracy of the theoretical approach discussed in this paper.

1. INTRODUCTION

In the Netherlands conditions are not always favourable to civil engineers. The western and northern parts of the country are below sea level, have poor subgrades and high water tables. Water management is a constant concern in these regions. Due to climate change and ongoing urbanisation the need for water storage capacity has increased in the last decade. Permeable pavements with a capacity to store and infiltrate water can contribute to solve some of the Dutch problems related to water. Permeable pavements should of course have ample bearing capacity to serve traffic.

The paper discusses a research into the bearing capacity of the Aquaflow permeable CBP system. First the mechanical properties (strength, stiffness and permanent deformation behaviour) of the unbound materials applied in the permeable CBP system were determined by means of triaxial testing, chapter 2. The observed material behaviour was then used as input for structural analyses. Combined, various calculations led to insight into the bearing capacity (i.e. rutting behaviour) of the permeable CBP, chapter 3. The results are verified against results from accelerated pavement tests reported in literature, chapter 4. The paper ends with conclusions in chapter 5.

2. MATERIAL BEHAVIOUR

2.1 Materials

Two materials have been tested. The first material is a 5/8 mm German limestone crusher run, CR 5/8, used in the bedding layer. Due to the absence of particles smaller than 5 mm CR 5/8 mm is highly permeable. The next material is an 8/32+ mm German limestone crusher run used as a granular base, GB 8/32+. The absence of particles smaller than 8 mm ensures that GB 8/32 is a highly permeable material. A special crushing process is adopted. This process ensures that the grain shape of CR 5/8 mm and GB 8/32+ is such that stable and compactable material is obtained.
Triaxial tests on CR 5/8 are performed at 100% DOC (degree of compaction). Given the structural importance of the base layer tests on the GB 8/32+ are performed at 97% and 104.5% DOC.
The triaxial tests that were performed are not discussed here. Reference is made to Sweere (1990), Huurman (1996a, 1997) and van Niekerk (2002).

2.2 Strength

The strength of unbound granular materials is well described by the failure criterion of Mohr-Coulomb.

$$\sigma_{1,f} = \frac{(1+\sin\phi)\sigma_{conf} + 2c\cos\phi}{1-\sin\phi} \qquad (1)$$

where:
c: cohesion [kPa]
ϕ: angle of internal friction [degr.]

σ_{conf}: confining pressure [kPa]
$\sigma_{1,f}$: first principal stress at failure [kPa]

Various failure static failure tests were done on the GB 8/32+ base material. The tests were done at 97.2% and 104.4% DOC. On the basis of linear interpolation and extrapolation of test results table 1 is obtained.

Also on the CR 5/8 failure tests are done. These tests are done at 100% DOC and led to the following strength properties: c= 8 kPa, Ø=47.7 degr.

Table 1. GB 8/32+ c and Ø as a function of density.

DOC [-]	γ_{dry} [kg/m^3]	c [kPa]	ϕ [degr.]	$\sigma_{1,f}$ @ 10 kPa [kPa]	$\sigma_{1,f}$ @ 100 kPa [kPa]
97%	1635.4	6.8	55.1	144.3	1053.3
98%	1652.3	12.0	55.5	181.0	1115.4
99%	1669.1	17.1	56.0	218.7	1179.7
100%	1686.0	22.3	56.4	257.5	1246.1
101%	1702.9	27.4	56.9	297.4	1314.9
102%	1719.7	32.6	57.3	338.6	1386.0
103%	1736.6	37.7	57.8	381.0	1459.7
104%	1753.4	42.9	58.2	424.8	1536.1
105%	1770.3	48.0	58.7	469.9	1615.2
106%	1787.2	53.2	59.1	516.4	1697.2
107%	1804.0	58.3	59.6	564.4	1782.4

2.3 Stiffness

In the triaxial test the stiffness is determined by application of a dynamic force controlled signal. Because of stress dependent behaviour the stiffness, Mr (resilient modulus), is measured at various stress combinations. Figure 1 gives the stiffness for GB 8/32+ measured at two DOCs. As indicated in the figure the stiffness of GB 8/32+ increases with compaction. The lines indicate the well known Mr-θ model.

$$Mr = k1\left(\frac{\theta}{\theta_0}\right)^{k2} \quad (2)$$

where:

Mr: resilient modulus [MPa]
k1: model parameter [MPa]
k2: model parameter [-]
θ: sum of principal stresses = $\sigma_1 + \sigma_2 + \sigma_3$ [kPa]
θ_0: reference stress =1 [kPa]

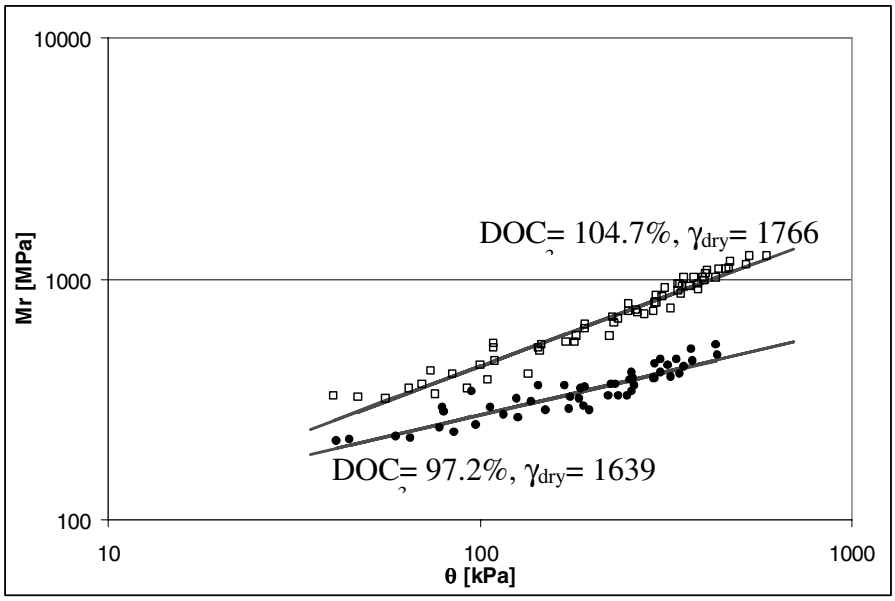

Figure 1. Graphical representation of measured and modeled Mr for GB 8/32+

Table 2. GB 8/32+ stiffness as a function of compaction and stress.

DOC [-]	γ_{dry} [kg/m3]	k1 [Mpa]	k2 [-]	Mr @ 100 kPa [Mpa]	Mr @ 1000 kPa [Mpa]
97%	1635.4	51.1	0.36	264.3	600.9
98%	1652.3	48.2	0.39	286.0	696.2
99%	1669.1	45.3	0.42	308.2	803.8
100%	1686.0	42.4	0.45	330.9	924.1
101%	1702.9	39.5	0.48	353.5	1057.5
102%	1719.7	36.6	0.51	375.7	1203.5
103%	1736.6	33.7	0.54	396.7	1361.1
104%	1753.4	30.8	0.57	415.8	1527.9
105%	1770.3	27.9	0.59	432.0	1699.9
106%	1787.2	25.0	0.62	443.9	1870.7
107%	1804.0	22.1	0.65	449.9	2030.8

By inter- and extrapolation of the measurements indicated in figure 1 table 2 was obtained.

Also the stiffness of CR 5/8 is measured. The stress dependent stiffness of finer (sand like) materials is better described with a model that distinguishes between the stiffness effects of σ_1 and σ_3, see equation (3).

For CR 5/8 at 100% DOC the following parameters are determined: k5= 13.35 MPa, k6=0.70, k7=0.17 and k8=8.63 (R^2=0.962).

$$Mr = k5\left(\frac{\sigma_3}{\sigma_0}\right)^{k6} \cdot \left(1 - k7\left(\frac{\sigma_1}{\sigma_{1,f}}\right)^{k8}\right) \quad (3)$$

where:

Mr:	resilient modulus [MPa]	σ_1:	first principal stress [kPa]
k5:	model parameter [MPa]	$\sigma_{1,f}$:	first principal stress at failure [kPa]
k6, k7, k8:	model parameters [-]	σ_3:	third principal stress [kPa]
		σ_0:	reference stress = 1 [kPa]

2.4 Permanent deformation

Unbound materials accumulate permanent strain under repeated loading. The rate of permanent strain accumulation is dependent on the state of stress, i.e. $\sigma_1/\sigma_{1,f}$. For the determination of the permanent deformation behaviour specimens are subjected to cyclic loading. Tests are done to a maximum of 1,000,000 cycles. All tests are done at $\sigma_3=\sigma_{conf}$ =12 kPa and 5 Hz (pulse width= 0.1 sec, rest period= 0.1 sec). To obtain insights into the stress dependency, tests are done at different levels of $\sigma_1/\sigma_{1,f}$.
The measured accumulation of permanent strain is described with.

$$\varepsilon_{perm} = A.\left(\frac{N}{1000}\right)^{B} + C\left(\exp\left[\frac{D.N}{1000}\right] - 1\right) \quad (4)$$

with

$$A = a1\left(\frac{\sigma_1}{\sigma_{1,f}}\right)^{a2} \text{ and } B = b1\left(\frac{\sigma_1}{\sigma_{1,f}}\right)^{b2} \text{ and } C = c1\left(\frac{\sigma_1}{\sigma_{1,f}}\right)^{c2} \text{ and } D = d1\left(\frac{\sigma_1}{\sigma_{1,f}}\right)^{d2}$$

where:

$\sigma_1/\sigma_{1,f}$:	stress ratio that equals 1 at failure [-]
a1, a2:	model parameters determining A as a function of $\sigma_1/\sigma_{1,f}$ [-]
b1, b2:	model parameters determining B as a function of $\sigma_1/\sigma_{1,f}$ [-]
c1, b2:	model parameters determining C as a function of $\sigma_1/\sigma_{1,f}$ [-]

d1, b2: model parameters determining D as a function of $\sigma_1/\sigma_{1,f}$ [-]

Figure 2 shows the results obtained from the permanent deformation tests on GB 8/32+ at 97% DOC. The figure shows four measurements; $\sigma_1/\sigma_{1,f}$= 0.57, 0.785, 0.88 and 1.02. As is indicated the tests done at $\sigma_1/\sigma_{1,f}$= 0.57, 0.785 and 1.02 follow the same trend, i.e. an increase in accumulated strain with an increase of $\sigma_1/\sigma_{1,f}$. The test done at $\sigma_1/\sigma_{1,f}$= 0.88 does not follow this trend and shows only limited deformation. For this reason the results obtained for $\sigma_1/\sigma_{1,f}$= 0.88 were not incorporated in the regression analysis that was done to obtain the parameters for the model given by equation (4).

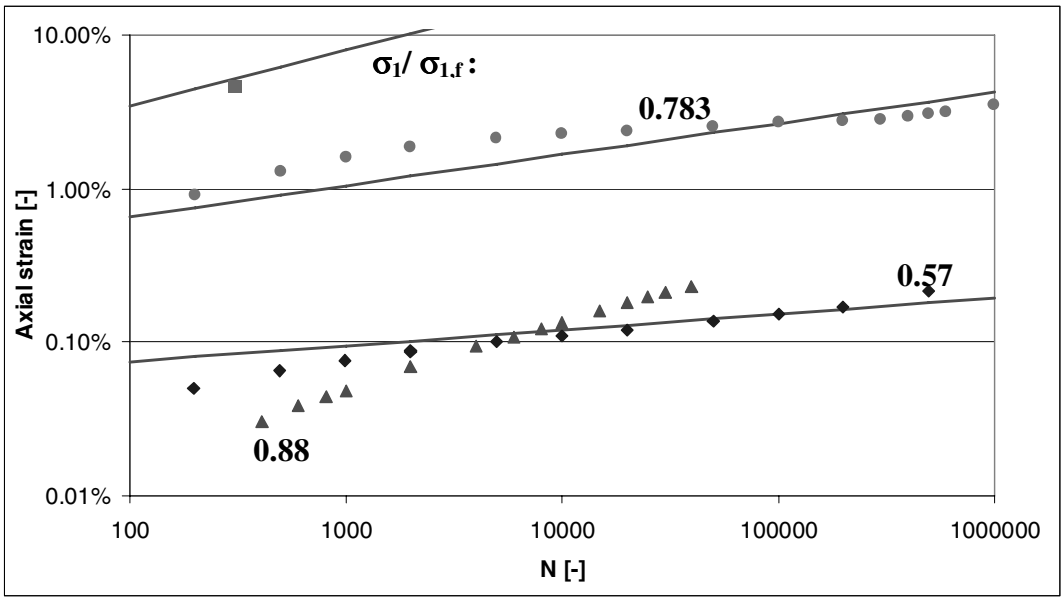

Figure 2. Permanent deformation for GB 8/32+ @ 97.0% DOC, measured axial strain and model.

Other permanent deformation tests, i.e. five tests on GB 5/32+ at 104.2% DOC and three tests on CR 5/8 at 100% DOC show similar results. The parameters describing permanent strain development in GB 8/32+ and CR 5/8 are given in tables 3 and 4 respectively. It is stated explicitly that table 4 was obtained by inter- and extrapolation on the basis of measurements at DOC 97.0% and DOC 102.2%.

Table 3 CR 5/8 parameters for the development of permanent strain @ 100% DOC.

	Axial permanent strain	Radial permanent strain
a1	-0.233%	0.256%
a2	15.84	19.27
b1	0.270	0.237
b2	2.985	7.768
C/D	c1=0, c2=1, d1=0, d2=1	
r^2	0.994	0.843

Table 4. GB 5/32+ parameters for the development of permanent strain as function of DOC and N.

	Axiaal							
DOC	a1 [-]	a2 [-]	b1 [-]	b2 [-]	c1 [-]	c2 [-]	d1 [-]	d2 [-]
97%	-6.80%	7.69	0.35	2.18	-2.73E-09	7.5	0.00	10
98%	-14.96%	6.96	0.51	2.05	-1.26E-08	7.5	0.03	10
99%	-20.27%	6.23	0.68	1.92	-4.64E-08	7.5	0.14	10
100%	-18.93%	5.51	0.82	1.79	-1.45E-07	7.5	0.65	10
101%	-13.10%	4.78	0.93	1.66	-4.02E-07	7.5	2.53	10
102%	-7.06%	4.05	0.99	1.53	-1.01E-06	7.5	8.65	10
103%	-3.08%	3.32	1.01	1.41	-2.35E-06	7.5	26.65	10
104%	-1.11%	2.60	0.99	1.28	-5.13E-06	7.5	75.52	10
105%	-0.34%	1.87	0.93	1.15	-1.06E-05	7.5	199.54	10
106%	-0.09%	1.14	0.86	1.02	-2.11E-05	7.5	496.96	10
107%	-0.02%	0.41	0.76	0.89	-4.02E-05	7.5	1176.80	10
	Radiaal							
DOC	a1 [-]	a2 [-]	b1 [-]	b2 [-]	c1 [-]	c2 [-]	d1 [-]	d2 [-]
97%	8.98%	9.83	0.40	2.72	2.33E-09	7.5	0.00	10
98%	31.03%	8.81	0.64	2.54	1.08E-08	7.5	0.03	10
99%	55.93%	7.79	0.88	2.35	3.96E-08	7.5	0.14	10
100%	61.01%	6.76	1.08	2.17	1.24E-07	7.5	0.65	10
101%	44.39%	5.74	1.21	1.98	3.43E-07	7.5	2.53	10
102%	23.04%	4.72	1.26	1.80	8.62E-07	7.5	8.65	10
103%	8.96%	3.70	1.23	1.61	2.01E-06	7.5	26.65	10
104%	2.70%	2.68	1.14	1.43	4.38E-06	7.5	75.52	10
105%	0.65%	1.66	1.01	1.24	9.08E-06	7.5	199.54	10
106%	0.13%	0.63	0.85	1.06	1.80E-05	7.5	496.96	10
107%	0.02%	0.00	0.69	0.87	3.44E-05	7.5	1176.80	10

3. CBP RUTTING BEHAVIOUR

3.1 Structural model

In pavements with unbound materials only, repeated traffic loading will lead to permanent deformation known as rutting. In stable pavements rutting develops slowly; guarantying a long design life. In unstable pavements rutting develops much faster; leading to a short design life.

Since the Aquaflow CBP-system is constructed with unbound materials only, ruts will develop under repeated traffic loading. Insight into the development hereof is required to enable proper structural design of the system. Hereto various structural Finite Element calculations were made. It is beyond the scope of this paper to fully describe the approach that was followed. However, hereafter the approach is briefly discussed, a detailed description may be found elsewhere (Huurman ,1997).

3.1.1. Material behaviour

The FE calculations that are at the basis of the structural analyses require material behaviour as input. Basically the calculations translate material behaviour into pavement behaviour by the use of structural modelling. For these three types of material behaviour are required as input: Strength, Stiffness and Permanent deformation behaviour. These inputs are as discussed in section 2.

3.1.2. Block layer

Individual blocks are interacting trough joints that are only mechanically active when compressed. The stiffness of the joints is determined from falling weight deflection measurements. Details hereof can be found elsewhere (Huurman, 1997).

3.1.3. Structural model

The structural model that translates material behaviour into pavement behaviour is a Finite Element model. The main features of this model are:

- Incorporated stress dependant material behaviour
- A block layer consisting of individual small elements that are interconnected by joints in which no tension can develop.

More details of the structural model can be found elsewhere (Huurman, 1996a,b,c, 1997)

3.2 Calculations

In total 53 calculations are made. The thickness of the sub-structure (i.e. bedding layer, base and sub base) equals 1000 mm in all cases. The thickness of the concrete blocks is not varied and equals 80 mm. Similarly the CR 5/8 bedding layer was 50 mm thick in all cases. The CR 5/8 bedding layer DOC was 100% in all cases.

The level of compaction of the GB 8/32+ base was varied between 97% and 105.5% DOC, the thickness of the GB 8/32+ base was varied (300, 400, 500 mm).
For the sub base inputs are based an average Dutch sand at DOC 100%. The sub-grade stiffness was not varied and equalled 60 MPa in all calculations.
Calculations are made for 30, 40 and 50 kN wheel loads, all applied via a circular area with a 150 mm radius (axle loads; 60, 80 and 100 kN).

3.2 Results

3.2.1 Rutting behaviour

From the analysis of individual calculation results it is observed that the permeable CBP system can display stable and unstable behaviour, see figure 3.

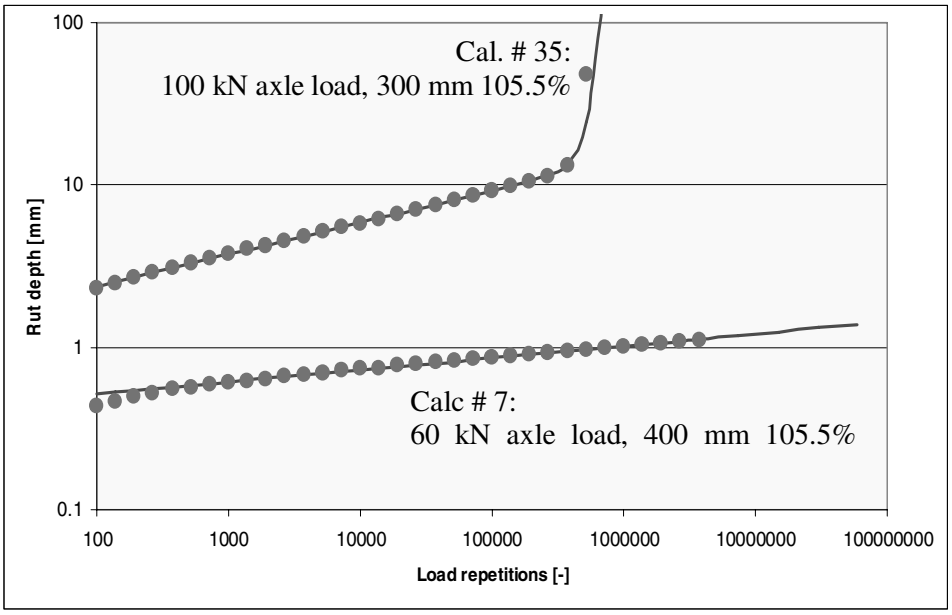

Figure 3. Examples of calculation results.

When the calculation results are put in perspective it is found that the 20 mm rut depth design life of the permeable pavement system increases with base compaction. For each combination of base thickness and axle load magnitude an optimum base DOC may be defined. After reaching this optimum DOC further compaction will not lead to further enlargement of the 20 mm rut depth design life. It is also found that the optimum base DOC increases with the axle load magnitude, see figure 4.

Furthermore it is found that the design life generally increases with base layer thickness, however, when axle loads become 100 kN this trend is broken. At lower levels of compaction, DOC <103 %, it is now observed that the design life decreases with base layer thickness. This indicates that the permeable base is not able to withstand repeated loading by 100 kN axle loads over a prolonged period of time when not compacted properly.

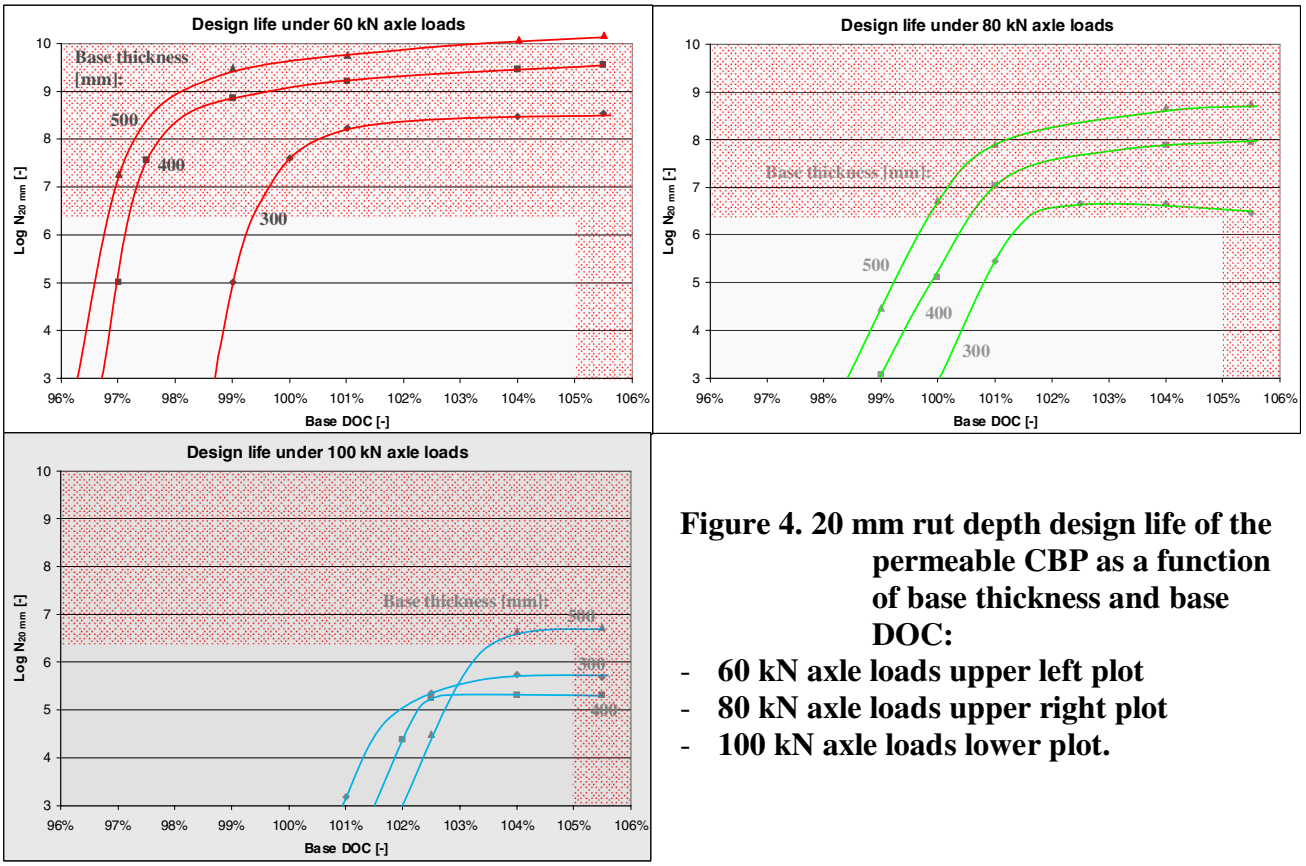

Figure 4. 20 mm rut depth design life of the permeable CBP as a function of base thickness and base DOC:

- **60 kN axle loads upper left plot**
- **80 kN axle loads upper right plot**
- **100 kN axle loads lower plot.**

When the base is well compacted (DOC >103%) the pavement design life under 100 kN axle loadings increases with base layer thickness. This indicates that a strong permeable CBP with unbound materials only can be obtained by application of a well compacted base with ample thickness.
The above indicates that base compaction is of the up-most importance for the structural behaviour of the permeable CBP-system.

3.2.2 Maximum axle load and verification

At TRL accelerated pavement tests have been performed on the English version of the Aquaflow pavement system (Atkinson and Blackman, 2001). The tests were done under repeated loading by a 57.5 kN wheel load, i.e. 115 kN axle load. Four test sections were tested, see table 5. All test sections were constructed over a clay subgade. On top of this subgrade a 500 mm thick 53% CBR capping layer was placed. Over this capping layer a 400 mm thick base was constructed. The base of section, C, consisted of a 10-63 mm limestone. In the sections A, B and D the lower 250 mm of the base consisted of 10-63 mm limestone while the upper 150 was 5-20 mm limestone. In all cases a 42-49 mm bedding layer was placed over the base. Furthermore the sections differed in terms of the use of geogrids.

Table 5. Summary of the accelerated pavement testing at TRL (Atkinson and Blackman, 2001).

Test section	A	B	C	D
DOC of upper 150 mm of the base [-]	99%	101%	n.a.	99%
DOC of lower 250 mm of the base [-]	106%	104%	109%	109%
Average DOC of base layer [-]	102.5%	102.5%	109%	104%
Rut depth after 7614 load repetitions [mm]	8.2	10	10.3	10.6
Rut depth after 15228 load repetitions [mm]			12.9	13.4
$N_{20\,mm}$ [-]	112168*	61636*	58763*	49768*

* *The TRL tests results and the calculations discussed here are put in perspective via 20 mm rut depth design life, $N_{20\,mm}$. $N_{20\,mm}$ is given in the last row of table 5 and is based on extrapolation of TRL test data on a log-log scale. Insight in this extrapolation is given in figure 5.*

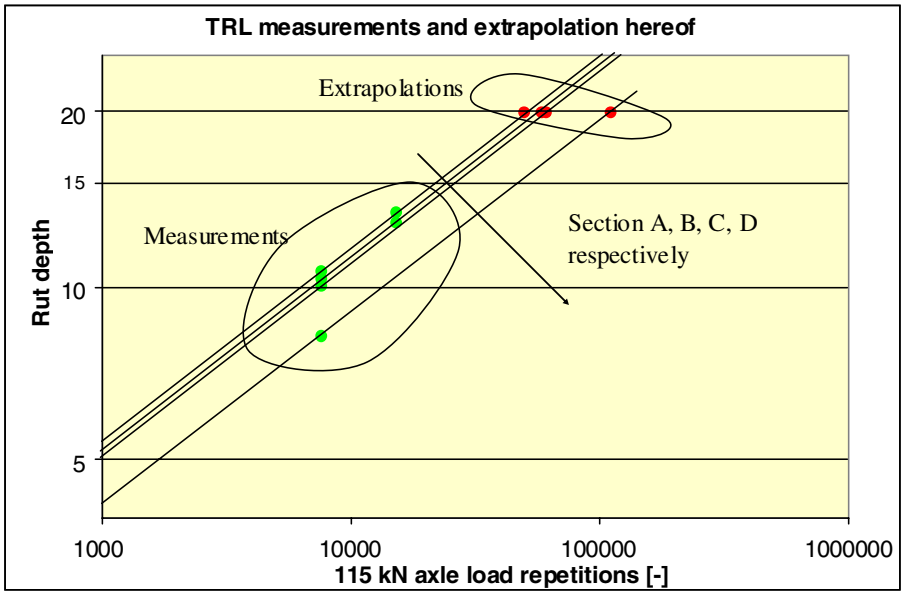

Figure 5. Extrapolation of TRL rut depth measurements.

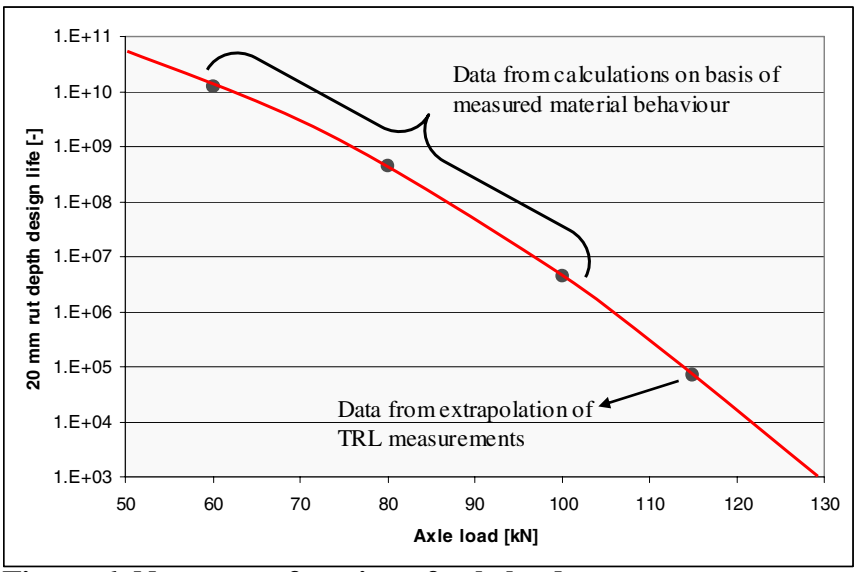

Figure 6. $N_{20\,mm}$ as a function of axle load (base 500 mm, 104% DOC)

The average DOC of the base in the TRL measurements was 104.5%. The average $N_{20mm\ for}$ 115 kN axle loadings is 70,500. The measurements of TRL consider a situation that is closest to calculations made for an Aquaflow pavement system with a 500 mm base at 104% DOC. Such calculations were made for the rutting behaviour under 60 kN, 80 kN and 100 kN axle loads. By combination of the calculation results and the TRL measurements figure 6 is obtained. The figure shows the 20 mm rut depth design life as a function of the axle load. The figure holds for systems with a 500 mm base at 104% DOC under fairly canalised traffic.

Figure 6 shows that the permeable CBP may be constructed so (base> 500 mm, DOC>104%) that it can resist axle loads of 105 kN over a prolonged period of time (N>10e6). With a further increase of the axle loads the design life decreases. Practically the maximum allowable axle load will be in the order of 120 kN to 130 kN. With this the

permeable CBP-system can be made strong enough to resist legal road going traffic in the Netherlands. Figure 6 furthermore indicates the good agreement between TRL measurements and the theoretical approach based on laboratory measurement and structural analysis discussed in this paper.

3.2.3 Strengthening the permeable CBP

When compared to "normal" Dutch base courses it is found that the GB 8/32+ has a high angle of internal friction and low cohesion. This implies that the material will be sensitive to lack of confinement. The effects of the observed material behaviour on the behaviour of the structure as a whole can best be understood by the development of stiffness. Figure 7 indicates the distribution of stiffness throughout the substructure of a permeable CBP loaded by a 60 kN axle load. The figure shows a stiffness distribution in the GB 8/32+ indicating a pressure dome like mode of load bearing.

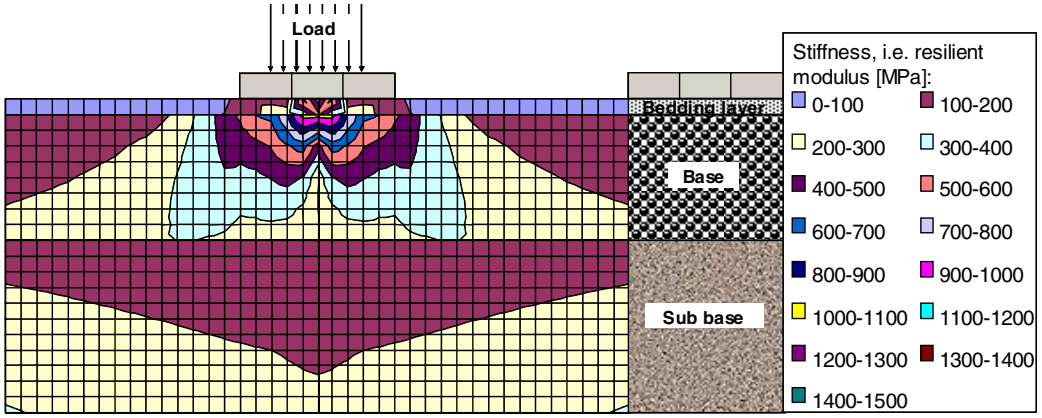

Figure 7. Stiffness of the substructure with a 400 mm base; 30 kN wheel load.

As indicated by figure 7 an area of low stiffness develops at the bottom of the GB 8/32+ base due to lack of confinement. With an increase of the axle load this low stiffness area grows upward. As a result the height of the stiff part of the base, i.e. the top of the dome, becomes smaller with an increase of axle load. At larger axle loads the height of this area has become too small. As a result the stresses in this area increase dramatically, leading to severe permanent strains and thus rutting at the pavement surface.

On the basis of the previous it is concluded that the bearing capacity of the permeable CBP may be increased when materials with larger cohesion are applied. These materials are less sensitive for lack of confinement. It is known from other research that cohesion in unbound materials follows mainly from the presence of finer fractions in the grading. Such fractions can however not be permitted in permeable pavements with water storing capacity. For this reason the bearing capacity of the permeable CBP may be increased by artificially increasing the cohesion. For this reason the application of a binder may be considered.

4. CONCLUSIONS

On the basis of the previous the following conclusions are drawn.

- The rut development in a permeable CBP determined by combination of laboratory measured material behaviour and a structural analysis is similar to the rut development measured in accelerated pavement tests.
- Due to the lack of fines the open graded base course material has limited cohesion.
- With increasing compaction the material gains cohesion, however even when well compacted cohesion remains limited.

- Due to this the bearing capacity of the permeable pavement with unbound materials only remains limited.
- However, with the application of well compacted base courses permeable concrete block pavements can be made strong enough to resist normal road traffic over a prolonged period of time.
- The maximum bearing capacity of a permeable CBP is in the order of 120 to 130 KN axle loads.
- It is expected that the bearing capacity of CBP can be further increased when the lack of base cohesion is compensated for, e.g. by application of a binder.

5. REFERENCES

Atkinson, V. and Blackman, D., 2001, Formpave: PTF Trial 2, Project report PR/IP/106/01, TRL Limited, England

Huurman M., 1996a, Resilient behaviour of concrete block pavements and the granular materials used in the substructure, Proceedings Pave Israel 96, The Fifth International Conference on Concrete Block paving, Tel-Aviv, Israel, 1996 pp. 239-251.

Huurman M., 1996b, Rut development in concrete block pavements due to permanent strain in the substructure, Proceedings Pave Israel 96, The Fifth International Conference on Concrete Block paving, Tel-Aviv, Israel, 1996 pp. 293-304.

Huurman M., 1996c, Structural design of concrete block pavements based on transversal and longitudinal unevenness, Proceedings Pave Israel 96, The Fifth International Conference on Concrete Block paving, Tel-Aviv, Israel, 1996 pp. 349-363.

Huurman, M., 1997, Permanent deformation in concrete block pavements, PhD Thesis, Delft University of Technology, Delft

Huurman M., L.J.M. Houben, C.W.A. Geense and J.J.M. van der Vring, 2003, The upgraded Dutch Design Method for Concrete Block Road Pavements, 7th International Conference on Concrete Block Paving, Pave Africa 2003, Sun City, South Africa 12- 15 October 2003.

Huurman, M., 2005, Mechanical behaviour of the Aquaflow pavement system, report 7-05-2001-31, Section of Road and Railway Engineering, Delft University of Technology, Delft, the Netherlands.

Huurman, M., 2005, Mechanical behaviour of the Aquaflow base and bedding material, report 7-05-2001-29, Section of Road and Railway Engineering, Delft University of Technology, Delft, the Netherlands.

Niekerk, A.A. van, 2002, Mechanical behaviour and performance of granular bases and sub-bases in pavements, PhD Thesis, Delft University of Technology, Delft

Sweere, G.T.H., 1990, Unbound granular bases for roads, PhD Thesis, Delft University of Technology, Delft